MINAR International Journal of Applied Sciences and Technology

Article type : **Research Article**

Date Received : **26/07/2021**
Date Accepted : **14/08/2021**
Date published : **01/09/2021**
: **www.minarjournal.com**
http://dx.doi.org/10.47832/2717-8234.3-3.12

SOLID CORE PHOTONIC CRYSTAL FIBER AS A BLOOD SERUM SENSOR BASED ON SURFACE PLASMON RESONANCE

Ahmed H. HADI[1], Soudad S. AHMED [2]& Firas S. MOHAMMED[3]

Abstract

In this work, a biomedical fiber sensor constructed of solid core optical photonic crystal fiber (SC-PCF)was fabricated to investigate different concentrations and the refractive index of blood serum samples based on surface Plasmon Resonance(SPR).In this study, the proposed structure was created by coating the first end of the photonic crystal fiber with a gold layer of 60 nm thickness. The second end of the photonic crystal fiber was connected to the multi-mode fiber (MMF). The obtained results show effective sensing performances. The sensors properties were measured; as the sensitivity equal to (11.11 μm/RIU), Signal to noise ratio (SNR) equal to 0.05and figure of merit (FOM) equal to 18.51. The fabricated SC-PCF biosensor can be used to measure efficiently the change in wavelength resonance caused by changing the concentration and refractive index of chemical and biological targets.

Keywords: Photonic Crystal Fiber, Bio-Sensor, Surface Plasmon Resonance.

[1] Mustansiriyah University, Iraq, ahmedahn2020@gmail.com
[2] Baghdad University, Iraq, soudadbassam@gmail.com
[3] Mustansiriyah University, Iraq, fsph@yahoo.com

Introduction

Based on its remarkable performance in fiber sensing based refractive index (RI), surface Plasmon resonance (SPR) has been broadly used in numerous domains, including environmental monitoring, bio sensing, medical development, and food safety[1].SPR in fiber optics have a wide academics' interest since it was created in 1993. In comparison to a standard prism SPR sensor, it offers more advantages such as; low cost, compact size and remote sensing suitability [2]. Depend on the RI variation several measurements can be employed for estimating the values of; bimolecular [3], pH value [4] and liquids concentration [5].When the transmitted light undergo total reflection inside the fiber, then an evanescent field generated and reach to the thin coated layer on the fiber's surface. Also, if the surface Plasmon wave (SPW) vector reaches the "phase matching condition" with the transmitted light wave vectors, then the charge density can oscillate at the metal-dielectric junction[6].Moreover, the cladding off [2], engraving [7], D-shape [8], tapering [9] and other manufacturing processes allowed additional evanescent waves move to the fiber surface and induce efficient SPR. Sensors built of photonic crystal fiber (PCF) have a simple design, cheap, and have excellent sensitivity and mechanical properties. The PCF's core due to the lack of cladding has a direct contact with the external environment and resulting in a multi-mode waveguide [10]. The oscillation of the electron density that accompanied with transverse magnetic (TM) along the polarized electromagnetic waves propagates parallel to the metal/dielectric contact [11].For SPR stimulation, the dielectric medium and the thin coated layer of metal overlaps the transmitted light has the same energy and velocity as the SPW. The energy of the photons and the metal electrons were connected to produce a substantial resonant drop in light intensity. The surrounding medium's RI is highly linked to SPW's propagation constant[12].To raise the evanescent wave, partial or total optical fiber cladding is eliminated in a standard SPR optical fiber sensor. Furthermore, the structural strength of the fibers was decreased by removing the cladding, thus the mechanical characteristics decreased. Moreover, to avoid fiber structural disturbance, sensitive SPR optical sensors can be created by employing grating structures. [13]. In this study, the properties of SC-PCF sensor have improved depending on coating the first end of the PCF with a gold layer and connecting the second end of PCF to the MMF. The fabricated PCF biosensor expected to be used to measure the concentration and RI of chemical and biological targets.

1. Photonic crystal fiber sensor concept

The optical fiber SPR sensor structure can be excited in different ways, including phase matching, polarizing the light parallel to the surface of metal, and sensing area inside the evanescent field. Typical evanescent field about 100–200 nm deep that decline exponentially from the junction of the fiber–gold layer. The light incidence angle, core and cladding RI are affected the evanescent field "penetration depth" (d) [14] as calculated in eq. (1):

$$d = \frac{\lambda}{\sqrt{n_1^2 \sin^2\theta - n_2^2}} \quad \ldots(1)$$

Where, λ is the wavelength of the incident light,n1 and n2 are the RIs of the fiber core and cladding respectively. The surface Plasmon polariton (SPP) propagation constant is stated as θ Represents the angle of incidence [15]:

$$\beta spp = \frac{\omega}{c}\sqrt{\frac{\varepsilon_s \cdot \varepsilon_m}{\varepsilon_s + \varepsilon_m}} \ldots(2)$$

Where ε_m and ε_s are the relative dielectric constants of gold layer and surrounding environment close to metal surface, respectively, c is the speed of light in vacuum and ω is the angular frequency of light. As a result, the phase-matching could be written as follows:[16]

$\beta i = \beta spp$ …(3)

where *i* is the fiber mode's order number of the propagation constant.

The resonance wavelength changes when the RI (or dielectric constant) of the surrounding environment changes, according to Eqs. (2) and (3). As a result, the sensing function may be possible to implement the performance aspects that will be evaluated include sensitivity, figure of merit, signal to noise ratio, and resolution. Sensitivity in spectral interrogation is defined as the change in resonance wavelength per unit change in the RI of the sensing material, and it is stated as [16]:

$$S = \frac{\Delta\lambda_{res}}{\Delta n_s}. \quad \text{…(4)}$$

The change in resonance wavelength is represented by $\Delta\lambda_{res}$,while the change in RI is represented by Δn_s. The unit of sensitivity determined from this equation is nanometers per RI unit (nm/RIU).The breadth of the SPR spectral curve is inversely proportional to the figure of merit (FOM) and signal to noise ratio (SNR), as shown in [16]:

$$FOM = \frac{S}{\Delta\lambda_{0.5}}. \quad \text{...(5)}$$

$$\mathrm{SNR}_{(n)} = \left[\frac{\Delta\lambda_{res}}{\Delta\lambda_{0.5}}\right]_n \quad \text{…(6)}$$

Where $\Delta\lambda_{0.5}$ is the width of the spectral curve.

The sensor resolution known as a detected variation in RI, and it is given as [17]:

$$\mathrm{R} = \frac{\Delta n_s}{\Delta\lambda_{res}}\Delta\lambda_{\mathrm{DR}}. \quad \text{…(7)}$$

Where ($\Delta\lambda_{\mathrm{DR}}$) is the spectrometer's spectral resolution.

2. Experimental work

The experimental setup is illustrated in Fig.(1). It consist of light source (halogen lamp), PCF (Thorlabs Co.),MMF, coupler, optical spectrum analyzer (OSA)(Thorlabs Co.) and computer. An OSA collects and analyzes the output spectrum, which is recorded and assessed by the computer.

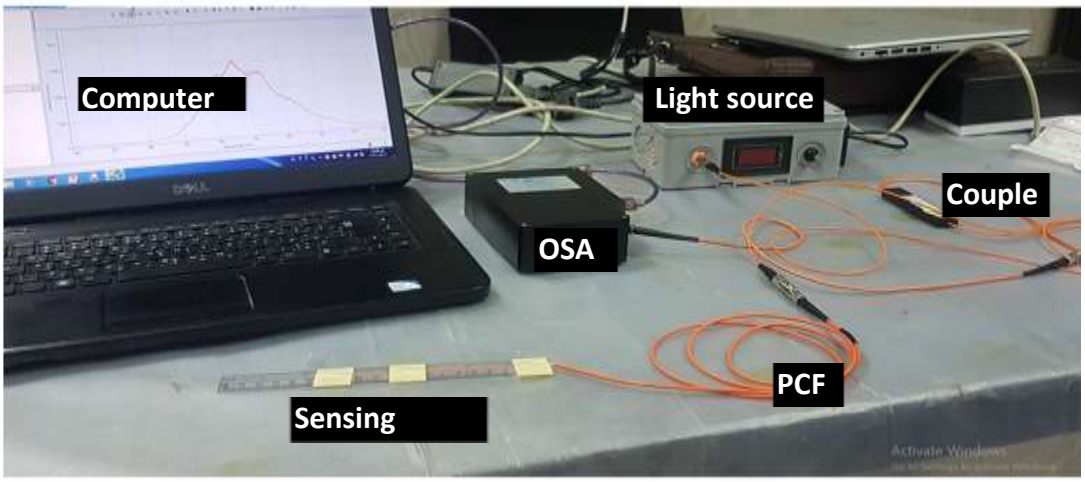

(a)

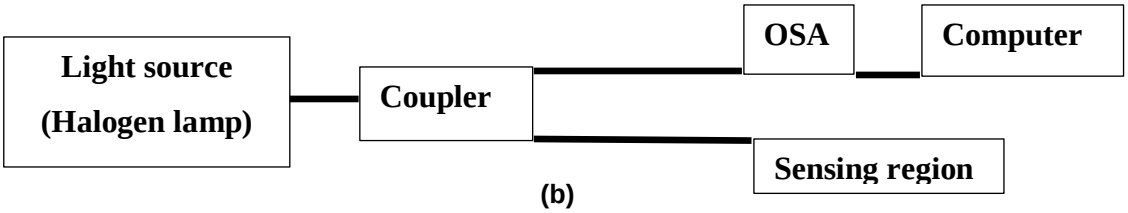

Figure 1. (a) Experimental setup, (b) Block diagram, of the proposed PCF sensor's structure based on SPR.

The optical fiber sensor preparation follows the following steps:

2.1 Optical fiber cleaning

The PCF is cut with a cleaver (CT-30) and the optical fiber connector (the end facesurface) cleaned with alcohol effectively, to avoid further contaminating the surface and provide the best possible result.

2.2 Optical sensor coating

The end surface of the fiber is coated with a gold layer of (60 nm) thickness by using the (Ion-Coater device) [COXEM: Model KIC-1A] that illustrated to make the PCF sensor. With a (20 mA) current and a (177 seconds) deposition time, the gold was deposited to a thickness of 60 nm. Fig.(4), depicts how the thicken works the thickness of the metal layer and it can be calculated by eq. (8)[19]

$$d=KIT \qquad \ldots(8)$$

Where d is the measured thickness. I is the current (20mA), K is the Constant number (0.17)and Tis the sputter time in second we made it (177 Sec.) for 60 nm layer.

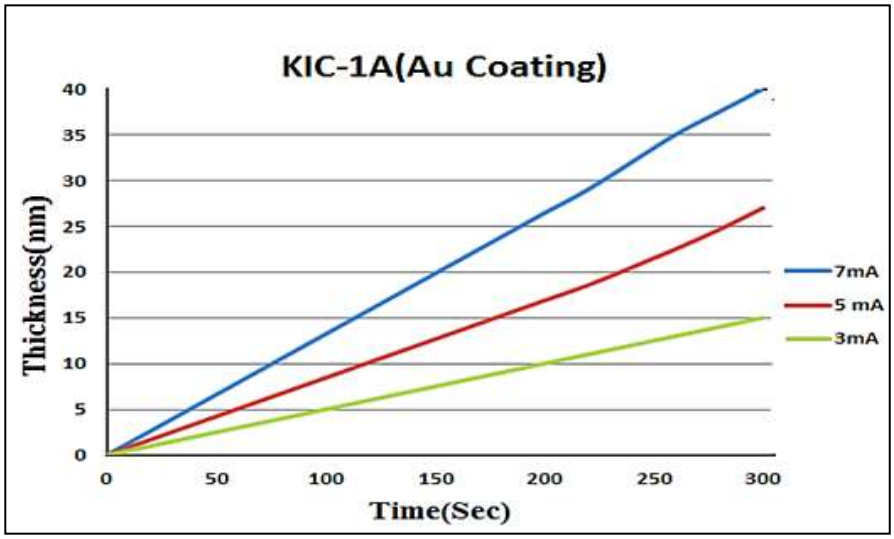

Figure2.The thickness of the coated gold layer as a function of time (sec.) [20].

The MMF is welded to a PCF by an ARC Fusion Splicer (Model: Fsm-60s)that used to join the two pieces.

2.3 Optical sensing implementation

The sensitive part of the sensor is subjected to a several sugar/water solutions of various concentrations, resulting in a range of refractive indices (n). An Abbe refract meter was used to determine the solutions' refractive indices.

3. Results and discussion

The performance of the sensor is estimated by immersing the coated end surface of PCFin the sugar/water solution to determine the solutions' refractive indices. Several solutions were prepared and their refractive indices were measured to be used as a reference for the sensing process .The linear relationship between RI and solution concentration is depicted in Figure 3.

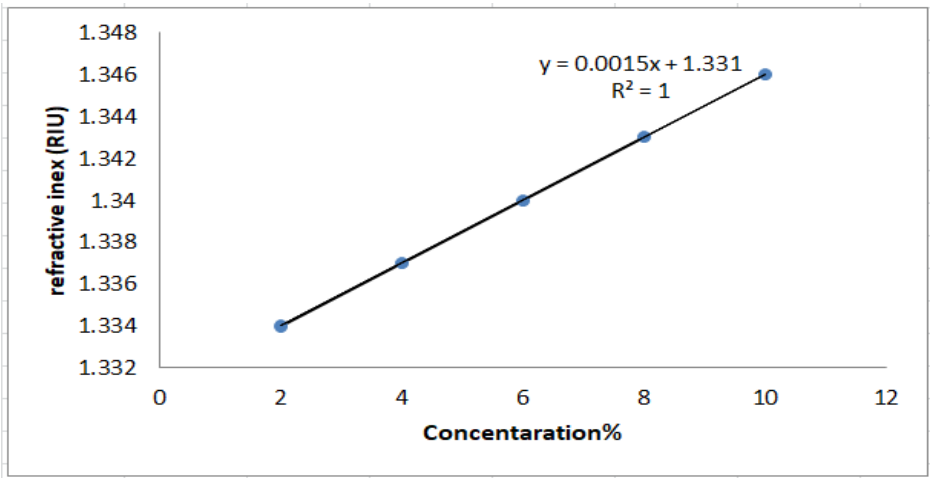

Figure 3.Sugar/water solutions' RI as a function of the concentration.

.

The sensing process done by using optical fiber sensor of 10mm length, the thickness of coated metal layer (d) of 60nm, varying RI values of (1.3426-1.3471) and PCF diameter (D)=125.3µm). As shown in Figure 6, the spectra are created by recording the transmission light curves (T) via an optical fiber. T can be calculated from dividing the optical signal intensity (Io) measured in the absence of a sample (sensing medium) by the intensity (I) measured in the presence of a sample (sensing media). The transmission (T) can be used as a function of wavelength (nm). The λ_{res} at a certain wavelength is labeled on the SPR curve, which is a T-wavelength curve. When the incident light's energy is transferred to the metal's electrons, T decreases dramatically, decreasing the intensity of the reflected light. The RI of the sensing material specifies when this dip occurs (n).The λ_{res} increases as the RI of the sensor medium increases. It generated from the resonance between and the SPR wave and the incident light. Moreover, as the energy level declines, the abrupt dip in the λ_{res} shifts to the longer wavelength side (red shift). It is illustrated that the higher the RI, the greater the λ_{res}.Also, at the lowest RI, the $\lambda_{res}$is (1.3426), and at the highest RI, the $\lambda_{res}$is (1.3471)as illustrated in Figure 4.

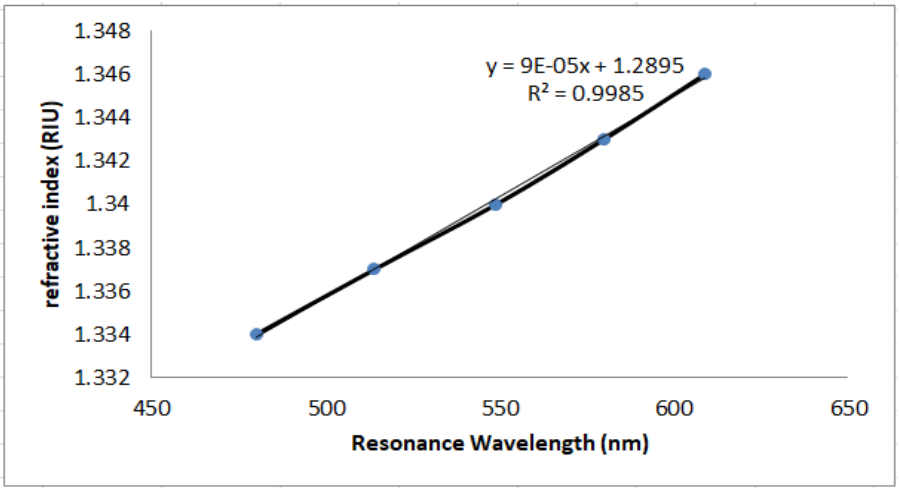

Figure4.The RI of a gold-coated sensor as a function of λ_{res} variation.

The sensor's SPR curves are shown in Figure 7. From the SPR response curve, it can be seen that for each sample there is different width and dip position i.e. any sample RI differ from the next, and the variation is clear in the regression position.

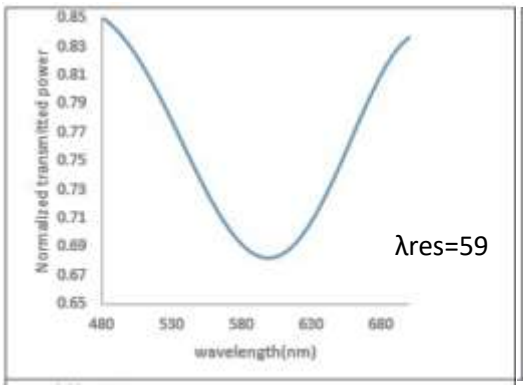

(a)

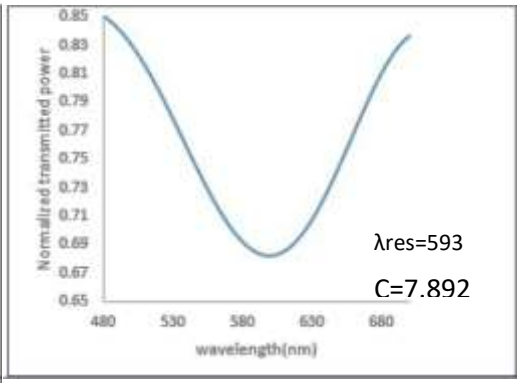

(b)

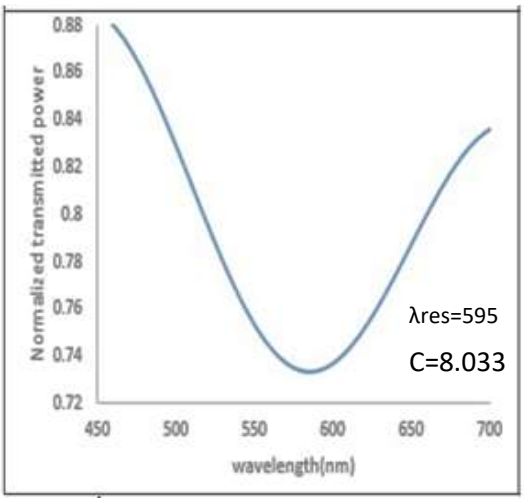

(c)

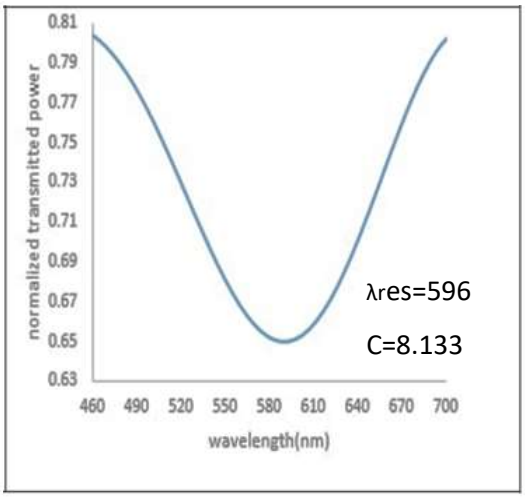

(d)

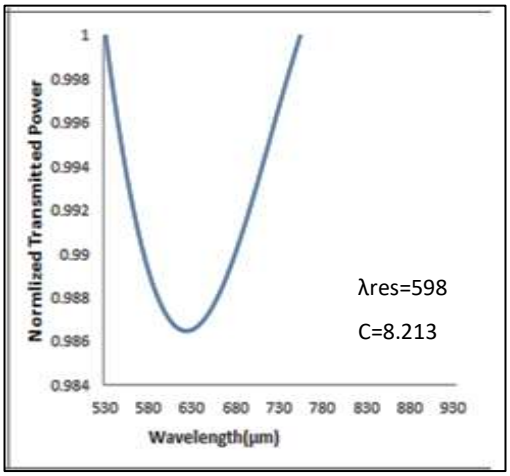

(e)

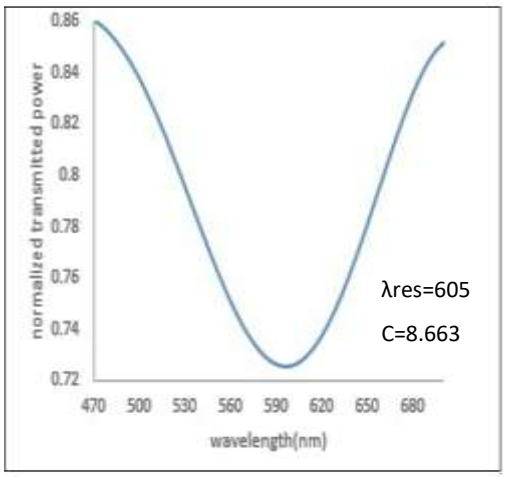

(f)

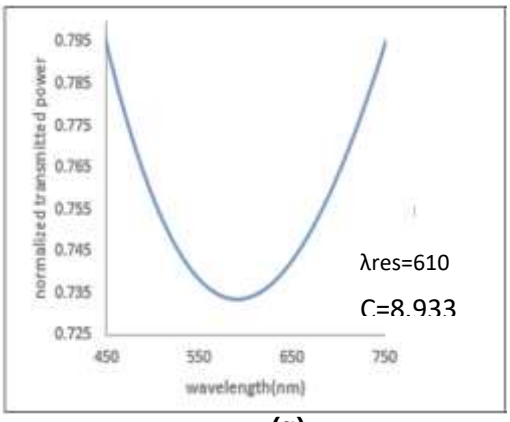

(g)

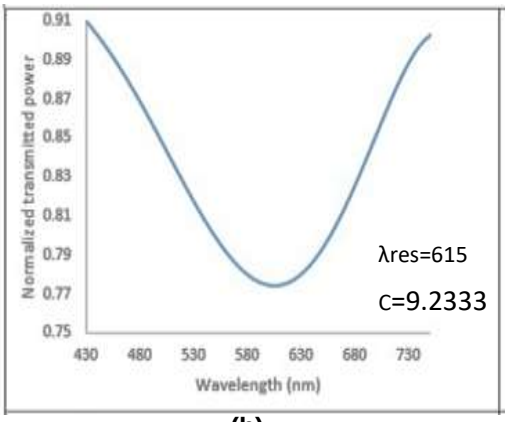

(h)

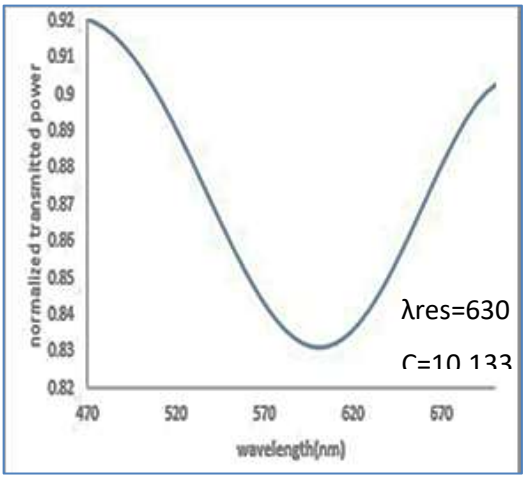

(i)

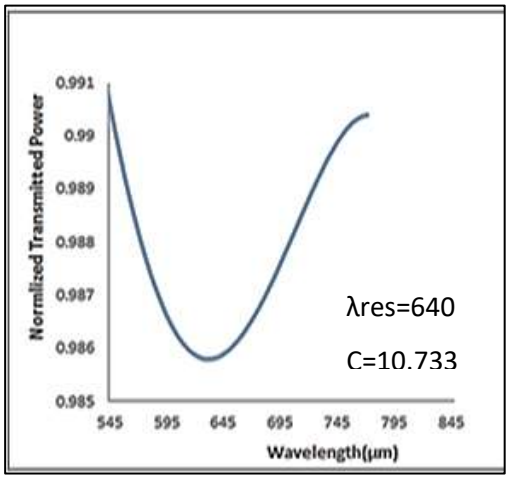

(j)

Figure 5. SPR curves of the proposed sensor without etching for different samples of blood serum.

Where the figure shows that the dip position of each SPR response curve is differed with the difference of the samples, i.e. with difference of the refractive index from one sample , and the difference is clear in the position of the regression, As the refractive index increases, the amplitude of the change in the dip position increases. When the resonance wavelength and refractive index of the sensing medium change, so do the performance characteristics, which are reliant on the surface Plasmon resonance (SPR) curve, shifting value, and dip position. The refractive index increases as the concentration of samples increases, and the lengths of the resonant wavelengths increase as a result, resulting in a strong shift to the red wavelength

Table (1) illustrates the values of the sensor's performance parameters.

The metal coating improve the sensitivity effectively, compare with PCF sensor with holes

Metal	Sensitivity (S_n) [μm/RIU]	(SNR)	(FOM)	Resolution [RIU]
Au	11.11	0.05	18.51	1.8x10^{-4}

based on SPR [21]. The proposed SC-PCF can be used as a good biosensor due to its high sensitivity and resolution, as it agree with [22].

4. Conclusion

As the refractive index rises, the resonance wavelength rises (strong shift to the red wavelength) due to an increase in the concentration of sugar in blood serum. The reason for this is that the sensing medium's refractive index is quite high because the real part of the wave vector of a surface Plasmon wave is higher than imaginary part. Thus, the resonance condition is fulfilled at longer wavelengths. It is clear from the results that for the optical fiber based on (SPR) sensor with a 60nm thick Au metal film and 1cm of exposed sensing region, success was achieved in obtaining effective performance parameters such as:the sensitivity is approaching 11.11m/RIU, SNRis 0.05, FOMis 18.51and the Resolutionis 1.8×10^{-4} RIU**.** The proposed SC-PCF can be used as a good biosensor**.**

References

A.K. Hassan,H.A.Yasur,and S.S. Al–Bassam,"Coreless Biomedical Optical Fiber Sensor

Ahmmed A. Rifat, Md. Rabiul Hasan, Rajib Ahmed and Haider Butt, " Photonic crystal fiber-based plasmonic biosensor with external sensing approach", J. Nanophoton. 12(1), 012503 (2017).

B.-T. Wang and Q. Wang, “Sensitivity-enhanced optical fiber biosensor based on coupling effect between SPR and LSPR,” *IEEE Sens. J.*, vol. 18, no. 20, pp. 8303–8310, 2018.

Based On Spr "Turkish Journal of Physiotherapy and Rehabilitation; 32(3)ol. 17,no.43,

H. Hu *et al.*, “High Sensitivity Fiber Optic SPR Refractive Index Sensor Based on Multimode-No-Core-Multimode Structure,” *IEEE Sens. J.*, vol. 20, no. 6, pp. 2967–2975, 2019.

J. G.Mohammed, and S. S. Al–Bassam. "Acetic acid concentration estimation using plastic optical fiber sensor based surface plasmon resonance." Iraqi Journal of Physics 17.43: 11-17(2019)

J. Homola, S. S. Yee, and G. Gauglitz, “Surface plasmon resonance sensors,” *Sensors actuators B Chem.*, vol. 54, no. 1–2, pp. 3–15, 1999.

M. Arjmand, H. Saghafifar, M. Alijanianzadeh, and M. Soltanolkotabi, “A sensitive tapered-fiber optic biosensor for the label-free detection of organophosphate pesticides,” *Sensors Actuators B Chem.*, vol. 249, pp. 523–532, 2017.

N. Cennamo, D. Massarotti, L. Conte, and L. Zeni, “Low cost sensors based on SPR in a plastic

optical fiber for biosensor implementation," *Sensors*, vol. 11, no. 12, pp. 11752–11760, 2011.

N. S. Rahim, "Estimating sugar concentration in human blood serum using Surface Plasmon Resonance (SPR)–based optical fiber sensor," *Iraqi J. Phys.*, vol. 17, no. 43, pp. 41–48, 2019.

N.S.Raham, and S.S. Al–Bassam, "Estimating sugar concentration in human blood serum using Surface Plasmon Resonance (SPR)–based optical fiber sensor". Iraqi Journal of Physics, 17(43): p. 41- 48. 2019.

P. T. Arasu, A. S. M. Noor, A. A. Shabaneh, M. H. Yaacob, H. N. Lim, and M. A. Mahdi, "Fiber Bragg grating assisted surface plasmon resonance sensor with graphene oxide sensing layer," *Opt. Commun.*, vol. 380, pp. 260–266, 2016.

Pibin Bing, Jialei Sui, Shichao Huang, Xinyue Guo, Zhongyang Li, Lian Tan, and Jianquan Yao, " A Novel Photonic Crystal Fiber Sensor with Three D-shaped Holes Based on Surface Plasmon Resonance", Current Optics and Photonics, Vol.3, No.6, 2019, pp. 541-547.

pp. 41–48, 2019

Q. Wang, B. Sun, E. Hu, and W. Wei, "Cu/ITO-coated uncladded fiber-optic biosensor based on surface plasmon resonance," *IEEE Photonics Technol. Lett.*, vol. 31, no. 14, pp. 1159–1162, 2019.

Q. Wang, J.-Y. Jing, and B.-T. Wang, "Highly sensitive SPR biosensor based on graphene oxide and staphylococcal protein a co-modified TFBG for human IgG detection," *IEEE Trans. Instrum. Meas.*, vol. 68, no. 9, pp. 3350–3357, 2018.

R. C. Jorgenson and S. S. Yee, "A fiber-optic chemical sensor based on surface plasmon resonance," *Sensors Actuators B Chem.*, vol. 12, no. 3, pp. 213–220, 1993.

R. Kant, R. Tabassum, and B. D. Gupta, "Fiber optic SPR-based uric acid biosensor using uricase entrapped polyacrylamide gel," *IEEE Photonics Technol. Lett.*, vol. 28, no. 19, pp. 2050–2053, 2016.

S. K. Srivastava and B. D. Gupta, "Influence of ions on the surface plasmon resonance spectrum of a fiber optic refractive index sensor," *Sensors Actuators B Chem.*, vol. 156, no. 2, pp. 559–562, 2011.

T. Guo, "Fiber grating-assisted surface plasmon resonance for biochemical and electrochemical sensing," *J. Light. Technol.*, vol. 35, no. 16, pp. 3323–3333, 2017.

T. Lang, B. Cao, C. Shen, and G. Shi, "Multimode-coreless-multimode fiber biosensor based on surface plasmon resonance," *J. Phys. D. Appl. Phys.*, vol. 52, no. 19, p. 195204, 2019.

Y. Al-Qazwini, A. S. M. Noor, Z. Al-Qazwini, M. H. Yaacob, S. W. Harun, and M. A. Mahdi, "Refractive index sensor based on SPR in symmetrically etched plastic optical fibers," *Sensors Actuators A Phys.*, vol. 246, pp. 163–169, 2016.

Y. Li, Y. Liu, Z. B. Liu, and S. S. Jian, "A refractive index sensor based on single-mode no-core single-mode fiber structure," *J. Optoelectron. Laser*, vol. 24, no. 7, pp. 1280–1285, 2013.

Y. Zhao, M. Lei, S.-X. Liu, and Q. Zhao, "Smart hydrogel-based optical fiber SPR sensor for pH measurements," *Sensors Actuators B Chem.*, vol. 261, pp. 226–232, 2018.